The levels of both lipid rafts and raft-located acetylcholinesterase dimers increase in muscle of mice with muscular dystrophy by merosin deficiency

María Teresa Moral-Naranjo, María Fernanda Montenegro, Encarnación Muñoz-Delgado, Francisco J. Campoy, Cecilio J. Vidal

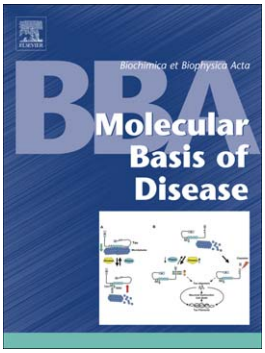

The levels of both lipid rafts and raft-located acetylcholinesterase dimers increase in muscle of mice with muscular dystrophy by merosin deficiency

María Teresa Moral-Naranjo, María Fernanda Montenegro, Encarnación Muñoz-Delgado, Francisco J. Campoy, Cecilio J. Vidal

PII: S0925-4439(10)00099-2
DOI: doi: 10.1016/j.bbadis.2010.05.011
Reference: BBADIS 63107

To appear in: *BBA - Molecular Basis of Disease*

Received date: 16 March 2010
Revised date: 12 May 2010
Accepted date: 26 May 2010

Please cite this article as: María Teresa Moral-Naranjo, María Fernanda Montenegro, Encarnación Muñoz-Delgado, Francisco J. Campoy, Cecilio J. Vidal, The levels of both lipid rafts and raft-located acetylcholinesterase dimers increase in muscle of mice with muscular dystrophy by merosin deficiency, *BBA - Molecular Basis of Disease* (2010), doi: 10.1016/j.bbadis.2010.05.011

The levels of both lipid rafts and raft-located acetylcholinesterase dimers increase in muscle of mice with muscular dystrophy by merosin deficiency

María Teresa Moral-Naranjo, María Fernanda Montenegro, Encarnación Muñoz-Delgado, Francisco J. Campoy, Cecilio J. Vidal*

Departamento de Bioquímica y Biología Molecular-A, Universidad de Murcia, Murcia, Spain

* Corresponding author: Dr. Cecilio J. Vidal.

Departamento de Bioquímica y Biología Molecular-A, Edificio de Veterinaria, Universidad de Murcia, Apdo. 4021, E-30071 Espinardo, Murcia, SPAIN.

Phone number: +34-868-884774, Fax number: +34-868-884147, E-mail: cevidal@um.es

ABSTRACT

Wild type and dystrophic (merosin-deficient) *Lama2dy* mice muscles were compared for their density of lipid rafts. The 5-fold higher level of caveolin-3 and the 2-3 times higher level of ecto-5'-nucleotidase activity in raft preparations (Triton X-100-resistant membranes) of dystrophic muscle supported expansion of caveolar and non-caveolar lipid rafts. The presence in rafts of glycosylphosphatidylinositol (GPI)-linked acetylcholinesterase (AChE) dimmers, which did not arise from erythrocyte or nerve, not only revealed for the first time the capacity of the myofibre for translating the AChE-H mRNA but also an unrecognized pathway for targeting AChE-H to specialized membrane domains of the sarcolemma. Rafts of dystrophic muscle contained a 5-fold higher AChE activity/mg protein. RT-PCR for 3'-alternative mRNAs of AChE revealed AChE-T mRNA prevailing over AChE-R and AChE-H mRNAs in wild type mouse muscle. It also displayed principal 5'-alternative AChE mRNAs with exons E1c and E1e (the latter coding for N-terminally extended subunits) and fewer with E1d, E1a and E1b. The levels of AChE and butyrylcholinesterase mRNAs were unaffected by dystrophy. Finally, the decreased level of proline-rich membrane anchor (PRiMA) mRNA in *Lama2dy* muscle provided for a rational explanation to the loss of PRiMA-bearing AChE tetramers in dystrophic muscle.

(195 words)

Keywords: caveolae; cholinesterases; ecto-5'-nucleotidase (CD73); muscular dystrophy

Running title: Acetylcholinesterase in lipid rafts

1. Introduction

Nearly half of patients (30-40%) suffering from congenital muscular dystrophy (CMD) shows a deficiency of the laminin-α2 chain (called merosin). Thus, the term 'merosin-deficient CMD' (MCMD) applies to the disease arising from anomalies in the *LAMA2* gene that encodes merosin [1,2]. *LAMA2* mutations affect laminin-2 (α2β1γ1) and laminin-4 (α2β2γ1). At the extracellular matrix laminin-2 links the sarcolemma through integrin α7β1D and α-dystroglycan, a protein of the dystrophin-glycoprotein complex that spanning the sarcolemma joins the extracellular matrix with the cytoskeleton of the myofibre. Laminin-2 is needed to seal the sarcolemma with the basement membrane. Its absence renders the sarcolemma fragile and permeable to calcium, and its increase leads to myofibre damage and muscle wasting [1,2]. Despite the above, the molecular etiopathogenesis of MCMD remains unsolved due to the variety of functions played by laminin-2. In humans and mice, MCMD leads to muscle degeneration and nerve dysmyelination [3], and, although several mouse strains (*Lama2dy*, dy^{2j}, dy^{w}, and dy^{3k}) are used for unveiling laminin-2 functions, the deficiency of merosin makes it the *Lama2dy* mouse a suitable model for MCMD studies [1].

Lipid rafts are membrane domains rich in cholesterol, sphingolipids and specific proteins, which have been shown to be involved in signal transduction [4]. The rafts are surrounded by less organized lipid/protein mixtures referred to as non-raft membranes [5,6]. Caveolae, the omega-shaped invaginations of the plasma membrane, are particular lipid rafts that contain the scaffolding protein caveolin (Cav) [7]; non-caveolar rafts are devoid of caveolin.

Acetylcholinesterase (AChE; EC 3.1.1.7) regulates synaptic and neurohumoral cholinergic activity by hydrolysing acetylcholine. Both 5' and 3'-alternatively spliced AChE mRNA variants have been identified [8,9]. 3' spliced mRNAs generate the three classical

AChE catalytic subunits, T, H and R [8,10]. AChE-T is by far the major and the most physiologically relevant subunit in mammalian brain and muscle. In muscle, AChE-T polymerizes into globular (G_1, G_2 and G_4) and asymmetric (A_4, A_8 and A_{12}) forms, which, after appropriate processing, reach specific cell stores [11,12]. The asymmetric species are the principal if not the only AChE forms in the neuromuscular junction (NMJ) of fast-twitch muscle [13]. The AChE-R subunit can replace the AChE-T protein in the oligomers of brain [8] and the AChE-H subunit incorporates glycosylphosphatidylinositol (GPI) and generates GPI-anchored G_1 and G_2 species [14]. Though functionally unrelated, AChE and ecto-5'-nucleotidase (eNT; CD73) share some properties. Both AChE-H forms and eNT lie in the cell membrane as GPI-linked dimers, where they hydrolyse neurotransmitters (acetylcholine and AMP) [15].

The importance of lipid rafts for membrane traffic [6] besides the increased number of caveolae in muscle of dystrophin-deficient mice [16] and of patients with Duchenne muscular dystrophy [17] prompted us to study firstly whether the merosin deficiency affected or not the population of lipid rafts in muscle. Moreover, bearing in mind: 1) the incorporation of GPI-linked proteins in lipid rafts [5]; 2) the presence in tissues of GPI-linked AChE-H protein; and 3) the role of rafts in targeting nicotinic receptors (nAChR) to the NMJ [18], our second goal was to look at the possible sorting of GPI-anchored AChE to lipid rafts as a means to justify the presence of AChE-H mRNA and protein in muscle and other tissues. Besides, given the abnormal pattern of AChE forms in merosin-deficient muscle [11] and the capacity of AChE to bind laminin, caveolin and other protein partners [19-21] it might be that the merosin deficiency disrupted AChE transport toward the surface membrane of muscle.

Since both caveolar and non-caveolar rafts exist, our third objective was to explore whether the content of non-caveolar rafts increased in merosin-deficient muscle. For this, advantage of the widely accepted use of catalytically active eNT as a marker of non-caveolar

rafts was taken [22,23]. Some of the results reported here have been published in a preliminary form [24].

2. Methods

2.1. Materials

Acetylthiocholine and butyrylthiocholine iodide, 5,5'-dithio-bis-2-nitrobenzoic acid, tetraisopropyl pyrophosphoramide (*Iso*-OMPA), 1,5-bis(4-allyldimethylammoniumphenyl)-pentan-3-one dibromide (BW284c51), AMP, α,β-methylene-ADP, Fiske-Subbarow reagent, 2-(N-morpholino)ethanesulfonic acid (MES), antiproteinases, polyoxyethylene$_{10}$-oleyl ether (Brij 96), sedimentation analysis markers (beef liver catalase, 11.4S, and alkaline phosphatase, 6.1S), Triton X-100, agarose-bound plant lectins, nitrocellulose membranes, peroxidase-conjugated anti-rabbit IgG (mAb A1949), anti-mouse IgG (pAb A9917) and anti-goat IgG (mAb A9452) were all provided by Sigma. Phosphatidylinositol-specific phospholipase C (PIPLC) from *B. thuringiensis* was kindly donated by Dr. Nigel M. Hooper (Univ. Leeds, UK). Primers for amplifying selected mRNAs were purchased from Invitrogen (Carlsbad CA, USA) and a PCR Master Mix from Applied Biosystems (Foster City CA, USA). The antibodies anti-Cav3 (mAb 610420) and anti-human AChE (mAb 610267) were from BD Biosciences (San Jose CA, USA). The rabbit antiserum against eNT of beef was a gift from Carlo Fini (Univ. Perugia, Italy). Alexa Fluor 488 goat anti-mouse IgG (pAb A11001) was from Molecular Probes (Eugene OR, USA). Western blots were developed by using the ECL Plus kit of Amersham Biosciences (Buckinghamshire, UK).

2.2. Isolation of lipid rafts

Breeding pairs of phenotypically normal (*Lama2* +/?) and dystrophic (*Lama2 dy/dy*; dystrophin-positive, merosin-negative) 129B6F$_1$/J mice were purchased from Jackson Labs. (Bar Harbor, ME, USA). Mice were kept and bred in the animal care unit of the University of Murcia and handled according to the Spanish legislation on 'Protection of Animals' and the Directives of the European Community. Lipid rafts of normal (NM) and dystrophic mouse muscle (DM) were isolated by their buoyancy in sucrose gradients essentially as reported elsewhere [25]. Normal and dystrophic mice, three months old and without sex distinction, were deeply anaesthetised with ether before heart perfusion with 5.4 mM EDTA, 154 mM NaCl, pH 7.4. Then, the hind limb muscles were excised and homogenized (20% w/v) in MES-buffered saline (MBS; 150 mM NaCl in 25 mM MES, pH 6.5) supplemented with 1% Triton X-100 and a cocktail of antiproteinases made of bacitracin (1 mg/ml), benzamidine (2 mM), pepstatin A (10 μg/ml), leupeptin (20 μg/ml), aprotinin (20 U/ml) and soybean trypsin inhibitor (0.1 mg/ml). The muscle was ground in Ultra-Turrax at low speed, five times for 10 s with 40 s intervals, and then in a glass-glass Potter (10 strokes). After centrifugation at 4ºC (5 min at 1,000 x g) the supernatant was mixed with its volume of 80% sucrose in MBS. The mixture (4 ml) was placed on centrifuge tubes and, after adding a 30-5% continuous sucrose gradient over the mixture, the tubes were centrifuged at 165,000 x *g*, for 16-20 h at 4ºC, in a SW41 Beckman rotor. Twelve fractions of 1 ml were collected from the top of the gradient and the Triton-resistant membrane fractions, containing the lipid rafts, were identified by their content in the protein markers of caveolar or non-caveolar rafts, i.e., Cav3 and eNT activity. More than 95% of the protein remained within the 40% sucrose layer, which contained the Triton X-100-soluble membranes. Fourteen raft preparations of NM and twelve of DM were analyzed.

2.3. Western blot analysis

Possible variation between NM and DM in the content of the raft markers Cav3 and eNT was assessed by Western blot. The presence of AChE in rafts was also tested. For this, 10 μg of protein of each gradient fraction was subjected to SDS-PAGE in 7.5% or 12.5% polyacrylamide gel slabs [26]. Occasionally two fractions were mixed to reach 10 μg of protein. After transfer, the nitrocellulose sheets were soaked in primary antibodies (1:1,000) and suitable peroxidase-conjugated antibodies. Blots were developed using ECL Plus. For semiquantitative estimation of the difference in Cav3 levels between NM and DM, the Cav3-rich membrane fractions were pooled, diluted three-fold with MES-buffered saline, centrifuged 15 min at 14,000 x *g*, and Western blotted. The intensity of ECL signals was measured with a Typhoon 9410 Imager (Amersham Biosciences) and a Microm image processing MIP 4.5 software (CID, Barcelona, Spain). In each Western blot assay, one normal and one dystrophic sample were compared, assigning a value of 1 to the total signal intensity of the raft fraction of normal muscle. Statistical analysis was performed by the Student's t-test.

2.4. Immunolabelling of Cav3 in muscle sections

Frozen muscle sections (0.4-0.5 mm thick) were fixed in buffered 4% paraformaldehyde, washed three times with a saline phosphate buffer, incubated with 0.1% Triton X-100 in the above buffer for 1 h, and washed again. After blocking with 3% bovine serum albumin in phosphate buffer, muscle sections were soaked overnight in anti-Cav3 antibodies (1:300) washed and incubated with Alexa Fluor 488 goat anti-mouse IgG (1:1,000). The slides were observed under a Leica TCS SP2 AOBS confocal module equipped with an HCX PLAN APO-CS 40.0 x 1.25 oil immersion lens. Confocal images

were obtained by excitation with an Ar laser at 488 nm and an emission of 519 nm for Alexa Fluor 488. For image analysis, the mean integrated optical density of 10 microscopic fields of NM and DM sections was recorded using a Microm image processing MIP 4.5 software. Statistical differences between normal and dystrophic muscle sections in Cav3 labelling were examined by the Mann-Whitney rank sum test.

2.5. Enzymatic assays

eNT activity was assayed with 1 mM AMP and the released phosphate was determined with a mixture of ammonium molibdate and Fiske-Subbarow reagent [27]. One unit of eNT activity (U) is the amount of enzyme that hydrolyzes one nmol of AMP per min at 37°C.

Cholinesterase (ChE) activity in the gradient fractions was assayed by the Ellman method [11]; AChE with 1 mM acetylthiocholine plus 50 µM *Iso*-OMPA and BuChE with 1 mM butyrylthiocholine plus 10 µM BW284c51. Inhibition of BuChE activity by Triton X-100 was relieved by adding 0.5% Brij 96 to the assay mixture. ChE activity is given in arbitrary units, one unit referring to an increase of 0.001 absorbance units per microliter of sample, and per minute. In sedimentation analysis, ChE activity was normalized for the volume of sample loaded onto the gradient. Activity values for NM and DM were compared by the Mann-Whitney rank sum test.

2.6. Identification of AChE forms located at lipid rafts

Fractions with lipid rafts were pooled and centrifuged. The pellet was extracted with a Tris-Triton X-100 buffer (150 mM NaCl, 5 mM EDTA, 60 mM octyl-glucoside, 1% Triton X-100 in 10 mM Tris-HCl, pH 8.0). Fractions with Triton-soluble membranes were also pooled and dialyzed in MBS for sucrose removal. AChE and BuChE forms in the Triton-

resistant and Triton-soluble membranes were resolved by sedimentation analysis. For this, samples and sedimentation markers were loaded on 5-20% sucrose gradients containing 0.5% Brij 96. After centrifugation at 165,000 x *g*, 20 h at 4ºC in a SW41 Beckman rotor, fractions were collected from the tube bottom, assayed for AChE and BuChE activities, and sedimentation coefficients of AChE forms were calculated [28]. The presence of GPI in the raft-bound AChE forms was tested by incubating samples with PIPLC (3 U/ml), 2 h at 37ºC. Removal of the hydrophobic domain in GPI-linked AChE was assessed by sedimentation analysis.

2.7. Lectin interaction assays

Lectin binding assays were used for testing possible differences between oligoglycans linked to homologous AChE forms in erythrocyte and lipid rafts of muscle. For this, lipid raft extracts (0.5 ml) were mixed with the same volume of Sepharose 4B (control) and of agarose-linked *Lens culinaris* agglutinin, wheat germ agglutinin and *Ricinus communis* agglutinin. After overnight incubation, agarose-bound AChE was removed and unbound AChE activity was quantified by sedimentation analysis [11].

2.8. Real time PCR for measuring the relative content of ChE mRNAs

Possible changes in the content of ChE mRNAs as the result of muscular dystrophy were examined by RT-PCR, using five NM and five DM samples. Details of RNA extraction from muscle and of assessment of its higher amount in DM than NM have been reported elsewhere [29]. For reverse transcription, 5 µg of total RNA (pre-treated with DNase I) was heated 10 min at 70ºC and cooled. A mixture of buffer, dNTPs, dithiothreitol, random primers and ribonuclease inhibitor was added, and all heated 2 min at 42ºC. Then, 200 units

of MMLV reverse transcriptase were added and cDNA synthesis performed at 42ºC for 50 min in a volume of 20 µl. Finally, cDNA samples were heated at 70ºC for 15 min.

PCR primers (Fig. 1) were designed for amplifying specific cDNAs that contained one of the five alternative exons (E1a, E1b, E1c, E1d and E1e) at the 5' region of the *ACHE* gene [8,9], as well as for amplifying the three cDNAs arising from the 3' spliced AChE mRNAs (R, H and T), and PRiMA, BuChE and β-actin mRNAs. For amplification we used an Applied Biosystems 7500 Real-time PCR machine and a MicroAmp Optical 96-well Reaction Plate with 25 µl of reaction volume, containing 2 µl of variable dilutions of cDNA, 0.2 µM of specific primers and a PCR Master Mix from Applied Biosystems. Reactions included a first step of 10 min at 95ºC, and 45 cycles of 15 s at 95ºC and 60 s at 60ºC. A final dissociating step was added to analyze the melting curves. The mRNA contents in NM and DM were compared using the Mann-Whitney rank sum test. PCR products were resolved in 3% agarose gels and revealed with ethidium bromide. Their size was calculated with DNA size markers (Sigma) and the GelPro software.

3. RESULTS

3.1. The content of caveolin-3 increases in merosin-deficient mouse muscle

Lipid rafts (Triton-resistant membranes) of muscle were isolated taking advantage of their insolubility in Triton X-100 and buoyancy in sucrose gradients. The rafts of NM concentrated in a sharp band (N1) in fractions 6-8 of the gradient (out of 12; supplementary Fig. S1A) and the rafts of DM distributed between a strong band (D1) in fractions 6-8 and a faint band (D2) in fractions 3-5. Per gram of muscle, 1.9 ± 1.1 mg of protein was recovered in N1 (n = 14), 3.4 ± 2.3 mg in D1 and 0.19 ± 0.07 mg in D2 (n = 12) (Fig. 2A). N1, D1 and D2 contained Cav3 (Fig. 2B), and the double quantity of protein in D1+D2 (3.6 ± 2.3 mg)

compared with N1, along with the nearly 5 times (4.8 ± 1.6, n = 6, p <0.001) stronger Western blot signal for Cav3 in rafts of DM than of NM (Fig. 2C) demonstrated enrichment of Cav3 and presumably of caveolae in merosin-deficient muscle. The 5-fold increase (5.1 ± 2.6, n = 4, p <0.001) in the immunofluorescence signal for Cav3 in DM sections compared to that in NM slices (Fig. 2D) lent strong support to the proposal.

3.2. Catalytically active eNT prefers raft membranes and inactive eNT non-raft membranes

Since the floating membranes likely consist of Cav3-free and Cav3-bearing rafts (non-caveolar and caveolar rafts), we next investigated whether the production of the former was boosted by the deficiency of merosin. For this, we exploited the consideration of eNT activity as a marker of non-caveolar rafts [22,23]. The fact that both eNT activity and Cav3 concentrated in the same membrane fractions of NM (Fig. 3) supported co-migration of caveolar and non-caveolar rafts, an idea corroborated by the increased levels of both Cav3 and eNT activity (2.3 ± 0.6 times, n = 5, p = 0.038) in the raft-rich fractions of DM (Fig. 3). Although eNT activity was confined to rafts, Western blots detected eNT protein in fractions with and without rafts (Fig. 3B). According to our previous results [29], the bands at 68-72 kDa in the gel lanes with rafts of NM (rich in eNT activity) should correspond to active eNT and the triplet at 72-78 kDa in non-raft fractions (lacking activity) to inactive eNT. Whilst non-catalytic eNT protein was similarly labelled in non-rafts of NM and DM (Fig. 3) both eNT activity and eNT protein (blot signal) rose in rafts of DM (2.3 ± 0.6 and 3.4 ± 1.3 times (n = 4, p = 0.017), respectively), and this confirmed previous observations concerning the relationship between muscular dystrophy and the increase of eNT activity in muscle [29].

3.3. Raft microdomains of muscle contain AChE activity

The reports showing interaction of AChE with Cav1 [21] and the need of caveolae for directing rapsyn/nAChR to the sarcolemma [18] prompted us to explore the presence of ChEs in rafts of muscle. Although AChE and BuChE activities were mostly measured in non-raft membranes (Fig. 4A), on the basis of the protein content in the collected fractions (ChE activity/mg of protein) a significant part of AChE activity (but no BuChE activity at all) was found associated with rafts (Fig. 4A). The nearly five-fold (4.6 ± 2.1, $n = 5$, $p = 0.024$) higher AChE activity/mg protein in rafts of DM than of NM (Fig. 4A) revealed a link between the density of rafts and the level of raft-bound AChE activity, while the unequal distribution of AChE activity and Cav3 in the raft-containing fractions (Fig. 4B) pointed to a preference of AChE for non-caveolar rafts, an idea strongly supported by its enrichment in rafts of Caco-2 cells (authors' observations) that do not express Cav1 [30].

3.4. AChE located at lipid rafts of muscle consists of GPI-anchored dimers

The targeting of GPI-anchored proteins to rafts [5], the recent observation of GPI-anchored AChE in rafts of cultured neuroblastoma/glioma hybrid cells transfected with *Torpedo* AChE-H [40], and the identification of AChE protein (Fig. 4) and enzyme activity (Fig. 5) in rafts of muscle prompted us to examine whether the raft-bound AChE consisted of GPI-linked species. Sedimentation analysis revealed that raft membranes contained only amphiphilic AChE dimers (G_2^A forms), whereas non-raft membranes exhibited G_1^A, G_2^A and occasionally hydrophilic tetramers (G_4^H forms) (Fig. 5). The almost complete conversion of the raft-associated G_2^A AChE species into G_2^H forms with PIPLC (supplementary Fig. S3A) allowed us to identify for the first time GPI-anchored AChE dimers in lipid rafts of muscle. As regards their adsorption to lectins, the raft-residing dimers were fully bound by *Lens*

culinaris agglutinin and wheat germ agglutinin, and almost fully bound by *Ricinus communis* agglutinin (supplementary Fig. S3B). This lectin interaction pattern differed from the one displayed by AChE dimers of sarcoplasmic reticulum [11] and blood cells [14].

3.5. *The levels of AChE and BuChE mRNAs are unaffected and that of PRiMA mRNA decreases in merosin-deficient muscle*

A comparison of the content of AChE and BuChE mRNAs in NM and DM could improve current understanding on the capacity of muscle for expressing the range of AChE mRNAs that differ in the choice of transcription initiation sites and alternative splicing (Figs. 1 and 6). In addition, the study might unveil possible differences between normal and dystrophic muscle in the splicing pattern of the *ACHE* gene. Figure 6 shows that the AChE mRNAs with E1c and E1e exons prevail over those with E1d, E1b or E1a exons in mouse muscle, and the AChE-T mRNA over the AChE-R and AChE-H mRNAs. It is worth noting that the E1e-containing mRNA encodes for an AChE subunit with an N-terminal extension which potentially allows membrane anchorage. The levels of BuChE and PRiMA mRNAs exceeded those of AChE-R and AChE-H mRNAs. The lack of differences in the content of AChE and BuChE mRNAs between NM and DM contrasted with the sixteen-fold lower level of the PRiMA mRNA in merosin-deficient than in normal muscle (210 vs. 3500 copies; $n = 5$, $p < 0.001$; Fig. 6), which demonstrated for the first time down-regulation of PRiMA in dystrophic muscle.

4. Discussion

4.1. The content of caveolin-3 increases in merosin-deficient mouse muscle

The insolubility of lipid rafts in Triton X-100 and their flotation in sucrose gradients allowed us to isolate the lipid raft populations. They appeared as a single band (N1) in preparations of normal muscle and two bands (D1 and D2) in those of merosin-deficient dystrophic muscle (supplementary Fig. S1). The almost 5-fold higher Western blot signal for Cav3 in D1+D2 than N1 (Fig. 1C) and stronger Cav3 labelling in *Lama 2dy* mouse muscle sections (Fig. 1D) supported a relationship between the deficiency of merosin and, therefore, of laminin-2 in muscle and the up-regulation of Cav3. In addition, the increase of Cav3 in merosin-deficient muscle (this report) and dystrophin-deficient muscle [17,31] links muscular dystrophy with caveolae expansion and agrees with the dystrophic phenotype of the Cav3 over-expressing mouse [32].

The high level of cholesterol in dystrophic muscle [33], its influence on the size and shape of rafts [17] and its activating effect on Cav expression [34] might explain the recovery of two raft populations (D1 and D2) in merosin-deficient muscle and its increased content of Cav3. The role that Cav3 fulfils in myoblast fusion, the lower density of rafts as myofibres mature [35], the muscular damage produced by statins, that lower cholesterol level and, therefore, the caveolae population [36], and our data pointing to an expansion of caveolar and non-caveolar (see below) rafts in DM all agree with the postulated impairment of myofiber differentiation as a leading factor for muscular dystrophy [37]. In addition, the high level of calcium in dystrophic muscle [38] and its activating effect on caveolin synthesis [39] make the deregulation of calcium homeostasis a probable cause for the excess of Cav3 in dystrophic muscle.

4.2. The increase of raft-associated eNT activity supports expansion of non-caveolar rafts in merosin-deficient muscle

The resistance of eNT activity to detergent extraction [27], its absence from caveolae [40], and the higher eNT activity/mg of protein in rafts (Fig. 3A) than whole muscle [15] all agree with the consideration of eNT activity as a marker of non-caveolar rafts [22]. The rise of Cav3 and eNT activity in the Triton-resistant membranes of DM supports expansion of caveolar and non-caveolar rafts, and the raft localization of active eNT (that converts AMP into adenosine) as well as adenosine receptors and adenosine deaminase [41] gives functional significance to the increase of eNT activity in dystrophic muscle [15].

4.3. Lipid rafts of muscle contains GPI-anchored dimers

AChE of muscle has been thoroughly studied because this enzyme is required for the correct coupling of excitation with contraction. The overwhelming amount and functional relevance in muscle of the AChE-T subunit (compared with AChE-H and AChE-R subunits) have boosted research onto regulatory aspects of the AChE-T mRNA expression, translation, oligomerisation of AChE-T subunits, assembly with non-catalytic (structural) subunits, and transport of oligomers to specific stores of muscle [10]. In fast muscle, AChE occurs as A_{12} forms made of T subunits at the NMJ and as PRiMA-bearing tetramers (G_4^A species) at the sarcolemma, whereas in slow fibres appears as G_1, G_4^A, A_4 and A_8 forms at synaptic and non-synaptic areas [13,42].

As regards the translation of the muscle AChE-H mRNA, despite the long time elapsed since its observation [43], the lack of information on AChE-H protein challenged the capacity of muscle for translating the AChE-H mRNA. The identification of G_2^A AChE species in rafts of muscle and their conversion into G_2^H forms with PIPLC (supplementary Fig. S2A)

demonstrate for the first time that muscle can translate the AChE-H mRNA and the existence of an as yet undetected pool of raft-residing AChE-H protein in the form of GPI-anchored dimers. This pool of dimers had probably remained unnoticed in whole muscle studies owing to the greater quantity of AChE-T than of AChE-H tailored molecules. The concentration in rafts of the latter permitted their identification.

The raft-residing AChE-H dimers were fully bound by *Lens culinaris* agglutinin and wheat germ agglutinin, and almost totally by *Ricinus communis* agglutinin (suppl. Fig. S2B), this lectin binding pattern differing substantially from that displayed by AChE dimers of sarcoplasmic reticulum [11] and blood cells [14]. Thus, along with the report showing AChE in caveolin-free membranes of erythrocytes [44], the differences between the AChE dimers in rafts of muscle and in erythrocytes in PIPLC sensitivity and extent of lectin binding (suppl. Fig. S2) [14] ruled out a possible erythrocytic origin of the raft-bound AChE. Finally, the lower binding extent of *Ricinus communis* agglutinin with the AChE dimers of nerves [3] than of rafts (suppl. Fig. S3B) discarded their possible neural origin.

The abundance in whole muscle and internal stores of asymmetric and tetrameric AChE-T [11], which are lacking in rafts (Fig. 5), and the rise of AChE activity (as dimers) in rafts of DM suggested package of particular subsets of AChE forms in distinct transport vesicles for their delivery to particular subcellular compartments of the myofibre.

4.4. 5'-Alternative AChE mRNAs

Our RT-PCR results demonstrate that mouse muscle expresses all five 5' alternative AChE transcripts described to date and the three 3' alternative AChE-T, AChE-R and AChE-H mRNAs (Fig. 6). The mRNAs with exons E1c and E1e prevailed over those with exons E1d, E1b and E1a in mouse muscle (this work) and brain [9], and this prevalence allowed us to report for the first time the capacity of muscle and brain to express AChE

transcripts containing the E1e exon which encodes the N-terminal extension. Our mRNAs data agree with those of the Soreq's group, who also observed abundant E1c-containing transcripts in most mouse tissues, including muscle, and undetectable or very low levels of mRNAs with E1d, E1b and E1a in muscle [45]. The expression level of E1e mRNAs in mouse organs was not analyzed in that work. Nevertheless, the substantial amount of E1e mRNAs in mouse muscle with respect to the total AChE transcripts that we observe agrees with the presence in human brain of the homologous 5'-spliced mRNA variant [46]. Finally, the increasing abundance of AChE-H, AChE-R and AChE-T mRNAs in mouse muscle (Fig. 6) also coincides with previous observations [45].

The identification in mouse muscle (this work) and brain [9] of E1e-containing AChE mRNAs that translate into N-terminally extended AChE subunits and whose extension potentially allows membrane anchorage [8] points to the production of N-extended AChE variants in muscle and brain. With respect to muscle, the strong labelling in lipid rafts of the ~66-72 kDa double protein band (Fig. 4B) that has been assigned to human N-extended AChE protein [45] supports its production in mouse muscle. With respect to brain, it is worth mentioning the presence in human cortical neurons of both E1e-containing AChE transcripts and N-AChE-T protein and their increased levels in neurons of patients suffering from Alzheimer disease [46]. This report prompts for an investigation focused on the identification in tissues of the various N-extended AChE proteins and their functional roles. We shall undertake this study in the near future using selected cell lines and antibodies against the N-terminal domain of N-extended AChE.

The prevalence of AChE-T mRNA over AChE-R and AChE-H mRNAs in muscle (Fig. 6) confirms the need of AChE-T protein for appropriate functioning, and the lower quantity of AChE-T and PRiMA mRNAs in mouse muscle (~9,500 and 3,500 copies/million copies of β-actin mRNA) (Fig. 6) than brain (35,000 and 8,000 copies) [9] agrees with the functional

importance of G_4^A AChE (the PRiMA-linked tetramers) for brain. The identification of BuChE and PRiMA mRNAs in muscle confirms its capacity for making the G_4^A BuChE forms that probably support neuromuscular transmission in AChE-null mice, which lack the homologous AChE forms [47].

4.5. The PRiMA subunit is down-regulated in merosin deficient muscle

The comparable amounts of AChE and BuChE mRNAs in healthy and merosin-deficient muscle contrasted with the sixteen-fold lower level of the PRiMA mRNA in merosin-deficient than in normal muscle (Fig. 6). This down-regulation of PRiMA would explain the reported decrease of G_4^A AChE and BuChE in dystrophin-deficient and merosin-deficient dystrophic muscle [11,48]. The role of PRiMA in converting G_4 AChE into G_4^A forms, and, hence, in attenuating the synthesis of asymmetric AChE [42], might account for the similar levels of G_4^A AChE in dystrophic fast-twitch and normal slow-twitch muscles, that are lower than in healthy fast-twitch muscle [49]. Down-regulation of PRiMA may be inherent to dystrophy; it may arise from early myogenin synthesis [50] and its suppressive action on PRiMA [42]. The need of PRiMA for targeting G_4^A AChE to the cell membrane in differentiating neurons [51] could mean that the down-regulation of PRiMA is responsible for the loss of G_4^A AChE and BuChE in merosin-deficient nerves [3], but further work is needed to confirm this.

4.6. Possible significance of AChE located in muscle lipid rafts

The role of lipid rafts in targeting nAChR [52] and our data revealing raft-bound AChE highlight the importance of rafts in targeting cholinergic proteins. The higher content of raft-confined AChE activity (in the form of AChE-H dimers) in *Lama2dy* muscle compared to

wild type muscle (Figs. 4, 5, and supp. Fig. S3A) contrasts with their similar levels of AChE-H mRNA (Fig. 6). This increased level of raft-bound AChE activity may arise from: 1) release of mRNA-blocking micro-RNA; 2) faster translation; 3) improved posttranslational maturation, including folding of AChE-H polypeptides, efficiency of GPI addition, conversion of catalytically incompetent into catalytic molecules, evasion from proteolysis, dimerization and exit to the Golgi [10]; and 4) favourable incorporation therein of the glypiated AChE in rafts and further targeting to the sarcolemma. Elucidation of these possible reasons deserves further investigation.

Concerning the functional significance of raft-bound AChE, the presence of muscarinic receptors (mAChR) in lipid rafts of muscle [53,54] supports a role for raft-bound AChE in cholinergic responses. The increased level of AChE activity in rafts of dystrophic muscle may contribute to the pathology by lowering the availability of acetylcholine. In addition, given 1) the non-enzymatic actions of AChE [10]; 2) its capacity to interact with laminin [19,20,55]; and 3) the similar structural motifs in AChE, syndecans, perlecans and other heparin sulfate proteoglycans [19], it is conceivable that the raft-bound AChE can contribute to the stabilization of the basal lamina of muscle.

4.7. Conclusions

The results reported herein demonstrate for the first time that the deficiency of merosin produces an increase in the content of Cav3 and of raft-bound eNT activity in muscle. These observations, besides the increased density of caveolae in dystrophin-deficient muscle [16,17], support the notion that regardless of the primary defect the dystrophic phenotype causes an increase in the population of caveolar and non-caveolar lipid rafts. The results are compatible with the notion of overproduction of lipid rafts in the damaged myofibre for

speeding up protein transport to the sarcolemma and activate repair. The identification of GPI-anchored AChE dimers in rafts of muscle justifies its content of AChE-H mRNAs and supports a role for rafts in delivering AChE toward the sarcolemma. Finally, the fact that PRiMA expression is down-regulated in merosin-deficient muscle would explain the loss of the physiologically relevant PRiMA-linked AChE and BuChE tetramers in dystrophic muscle.

Acknowledgments

This research was supported by the Ministerio de Ciencia y Tecnología of Spain (SAF2001/0279) and Fundación Séneca de la Comunidad Autónoma de la Región de Murcia (PI 83/00840/FS01). M.T.M.-N. and M.F.M. hold scholarships from CajaMurcia and the Fundación Séneca, respectively.

LEGENDS TO THE FIGURES

Fig. 1. Primers used in the PCR assays to quantify AChE, BuChE and PRiMA mRNAs. A) Scheme with the position of the primers. The 3' parts of p51, p53 and p55, which are complementary to E4, are only four nucleotides long. B) Primers sequences.

Fig. 2. Triton X-100-resistant lipid rafts were isolated from normal muscle (NM) and dystrophic muscle (DM) by isopycnic centrifugation. (A) Protein content in the gradient fractions. The inset shows the protein amount in the raft-rich fractions at an amplified scale. (B) Protein blots for Cav3 in the fractions, with 10 µg of protein per lane. (C) Relative content of Cav3 in lipid rafts. The membrane fractions rich in Cav3 were pooled, and the membranes were sedimented and subjected to Western blot. The total amount of protein loaded per lane is indicated. Please note that 5 µg of NM sample gave a much lower signal than 2 µg of DM sample. Quantitative analysis showed a five-fold higher content of Cav3 in rafts of DM than of NM. (D) Immunofluorescence analysis of normal and dystrophic muscle sections showing a 5-fold stronger labelling of Cav3 in merosin-deficient muscle ($p<0.001$). Scale bar = 150 µm.

Fig. 3. Distribution of eNT activity and eNT protein in raft and non-raft membranes of NM and DM. (A) eNT activity in fractions from the sucrose gradient. Note the greater eNT activity in DM than in NM, the confinement of the activity to rafts, and the higher specific eNT activity in raft membranes of dystrophic muscle. Plots show activity per milligram of protein (specific activity) and per volume. (B) Western blot with eNT protein in gradient fractions, with 10 µg of protein per lane. Note the difference in intensity and size of bands of eNT protein in raft and non-raft fractions.

Fig. 4. Identification of AChE in lipid rafts. (A) Distribution of AChE and BuChE activities in gradient fractions showing high specific AChE activity in lipid rafts and absence of BuChE activity from rafts. (B) Western blots with different banding patterns of AChE in raft and non-raft fractions (10 µg protein/lane). The strong labelling of AChE in raft fractions of DM agrees with their higher AChE activity.

Fig. 5. Sedimentation profiles with cholinesterase forms in raft and non-raft fractions of NM and DM. Raft membranes are devoid of BuChE activity. Sucrose gradients contained 0.5% Brij 96. C and P denote catalase and alkaline phosphatase.

Fig. 6. Expression of AChE, BuChE and PRiMA mRNAs. (A) Agarose gels showing the RT-PCR products for the 5' (E1a, E1b, E1c, E1d and E1e) and 3' (AChE-T, AChE-H and AChE-R) alternative mRNAs, as well as those for the BuChE and PRiMA mRNAs. (B) Histogram with levels of the mRNAs in NM and DM. The relative amounts of mRNAs are given as number of copies per million copies of the β-actin mRNA. Mean values of five NM and five DM samples. (*) Note the 16-fold lower level of the PRiMA mRNA in merosin-deficient muscle than in normal muscle ($p < 0.001$).

Supplementary Fig. S1. Isolation by isopycnic centrifugation of Triton X-100-resistant lipid rafts from normal muscle (NM) and dystrophic *Lama2dy* mouse muscle (DM). The bands N1, D1 and D2 observed at the middle of the gradient correspond to raft membranes.

Supplementary Fig. S2. Characterization of AChE dimers in lipid rafts of muscle. (A) PIPLC treatment demonstrating that they contain a GPI anchor. (B) Sedimentation profiles of the AChE activity which remained in the supernatant after removing lectin-AChE complexes. LCA, *Lens culinaris* agglutinin; WGA, wheat germ agglutinin; RCA, *Ricinus communis* agglutinin.

References

[1] C. Jiménez-Mallebrera, S.C. Brown, C.A. Sewry, F. Muntoni, Congenital muscular dystrophy: molecular and cellular aspects, Cell. Mol. Life Sci. 62 (2005) pp. 809-823.

[2] M.T. Lisi and R.D. Cohn, Congenital muscular dystrophies: new aspects of an expanding group of disorders, Biochim. Biophys. Acta 1772 (2007) pp. 159-172.

[3] M.T. Moral-Naranjo, J. Cabezas-Herrera, C.J. Vidal, F.J. Campoy, Muscular dystrophy with laminin deficiency decreases the content of butyrylcholinesterase tetramers in sciatic nerves of *Lama2dy* mice, Neurosci. Lett. 331 (2002) pp. 155-158.

[4] P. Lajoie, J.G. Goetz, J.W. Dennis, I.R. Nabi, Lattices, rafts, and scaffolds: domain regulation of receptor signaling at the plasma membrane, J. Cell Biol. 185 (2009) pp. 381-385.

[5] A.E. Garner, D.A. Smith, N.M. Hooper, Sphingomyelin chain length influences the distribution of GPI-anchored proteins in rafts in supported lipid bilayers, Mol. Memb. Biol. 24 (2007) pp. 233-242.

[6] M.F. Hanzal-Bayer and J.F. Hancock, Lipid rafts and membrane traffic, FEBS Lett. 581 (2007) pp. 2098-2104.

[7] R. Hnasko and M.P. Lisanti, The biology of caveolae: lessons from caveolin knockout mice and implications for human disease, Molec. Interventions 3 (2003) pp. 445-463.

[8] E. Meshorer and H. Soreq, Virtues and woes of AChE alternative splicing in stress-related neuropathologies, Trends Neurosci. 29 (2006) pp. 216-224.

[9] F.J. Fernández-Gómez, E. Muñoz-Delgado, M.F. Montenegro, F.J. Campoy, C.J. Vidal, J. Jordán, Cholinesterase activity in brain of senescence-accelerated-resistant mouse SAMR1 and its variation in brain of senescence-accelerated-prone mouse SAMP8, J. Neurosci. Res. 88 (2010) pp. 155-166.

[10] J. Massoulié, N. Perrier, H. Noureddine, D. Liang, S. Bon, Old and new questions about cholinesterases, Chem. Biol. Interact. 175 (2008) pp. 30-44.

[11] J. Cabezas-Herrera, M.T. Moral-Naranjo, F.J. Campoy, C.J. Vidal, Glycosylation of acetylcholinesterase forms in microsomal membranes from normal and dystrophic *Lama2dy* mouse muscle, J. Neurochem. 69 (1997) pp. 1964-1974.

[12] M. Guerra, A. Cartaud, J. Cartaud, C. Legay, Acetylcholinesterase and molecular interactions at the neuromuscular junction, Chem. Biol. Interact. 157-158 (2005) pp. 57-61.

[13] R.L. Rotundo, S.G. Rossi, L.M. Kimbell, C. Ruiz, E. Marrero, Targeting acetylcholinesterase to the neuromuscular synapse, Chem. Biol. Interact. 157-158 (2005) pp. 15-21.

[14] S. Nieto-Cerón, L.F. Sánchez del Campo, E. Muñoz-Delgado, C.J. Vidal, F.J. Campoy, Muscular dystrophy by merosin deficiency decreases acetylcholinesterase activity in thymus of *Lama2dy* mice, J. Neurochem. 95 (2005) pp. 1035-1046.

[15] M.S. García-Ayllón, F.J. Campoy, C.J. Vidal, E. Muñoz-Delgado, Identification of inactive ecto-5'-nucleotidase in normal mouse muscle and its increased activity in dystrophic *Lama2*^{dy} mice, J. Neurosci. Res. 66 (2001) pp. 656-665.

[16] P. Vaghy, J. Fang, W. Wu, L. Vaghy, Increased caveolin-3 levels in *mdx* mouse muscles, FEBS Lett. 431 (1998) pp. 125-127.

[17] S. Repetto, M. Bado, P. Broda, G. Lucania, E. Masetti, F. Sotgia, I. Carbone, A. Pavan, E. Bonilla, G. Cordone, M.P. Lisanti, C. Minetti, Increased number of caveolae and caveolin-3 overexpression in Duchenne muscular dystrophy, Biochem. Biophys. Res. Commun. 261 (1999) pp. 547-550.

[18] D. Zhu, W.C. Xiong, L. Mei, Lipid rafts serve as a signaling platform for nicotinic acetylcholine receptor clustering, J. Neurosci. 26 (2006) pp. 4841-4851.

[19] G. Johnson, C. Swart, S.W. Moore, Non-enzymatic developmental functions of acetylcholinesterase - the question of redundancy, FEBS J. 275 (2008) pp. 5129-5138.

[20] L.E. Paraoanu and P.G. Layer, Acetylcholinesterase in cell adhesion, neurite growth and network formation, FEBS J. 275 (2008) pp. 618-624.

[21] S.E. Park, S.H. Jeong, S.B. Yee, T.H. Kim, Y.H. Soung, N.C. Ha, N.D. Kim, J.Y. Park, H.R. Bae, B.S. Park, H.J. Lee, Y.H. Yoo, Interactions of acetylcholinesterase with caveolin-1 and subsequently with cytochrome *c* are required for apoptosome formation, Carcinogenesis 29 (2008) pp. 729-737.

[22] K. Matschke, E.B. Babiychuk, K. Monastyrskaya, A. Draeger, Phenotypic conversion leads to structural and functional changes of smooth muscle sarcolemma, Exp. Cell Res. 312 (2006) pp. 3495-3503.

[23] A. Ostapkowicz, K. Inai, L. Smith, S. Kreda, J. Spychala, Lipid rafts remodelling in estrogen receptor-negative breat cancer is reversed by histone deacetylase inhibitor, Mol. Cancer Ther. 5 (2006) pp. 238-245.

[24] M.T. Moral-Naranjo, M.F. Montenegro, E. Muñoz-Delgado, F.J. Campoy, C.J. Vidal, Targeting of acetylcholinesterase to lipid rafts of muscle, Chem. Biol. Interact. 175 (2008) pp. 312-317.

[25] F. Galbiati, J.A. Engelman, D. Volonte, X.L. Zhang, C. Minetti, M. Li, H. Hou, B. Kneitz, W. Edelmann, M.P. Lisanti, Caveolin-3 null mice show a loss of caveolae, changes in the microdomain distribution of the dystrophin-glycoprotein complex, and T-tubule abnormalities, J. Biol. Chem. 276 (2001) pp. 21425-21433.

[26] F. Ruiz-Espejo, J. Cabezas-Herrera, J. Illana, F.J. Campoy, E. Muñoz-Delgado, C.J. Vidal, Breast cancer metastasis alters acetylcholinesterase activity and the composition of enzyme forms in axillary lymph nodes, Breast Cancer Res. Treat. 80 (2003) pp. 105-114.

[27] A. Martínez-Martínez, E. Muñoz-Delgado, F.J. Campoy, C. Flores-Flores, J.N. Rodríguez-López, C. Fini, C.J. Vidal, The ecto-5'-nucleotidase subunits in dimers are not linked by disulfide bridges but by non-covalent bonds, Biochim. Biophys. Acta 1478 (2000) pp. 300-308.

[28] M.T. Moral-Naranjo, J. Cabezas-Herrera, C.J. Vidal, Molecular forms of acetyl- and butyrylcholinesterase in normal and dystrophic mouse brain, J. Neurosci. Res. 43 (1996) pp. 224-234.

[29] J.C. Morote-García, L.F. Sánchez del Campo, F.J. Campoy, C.J. Vidal, E. Muñoz-Delgado, The increased ecto-5'-nucleotidase activity in muscle, heart and liver of laminin α2-deficient mice is not caused by an elevation in the mRNA content, Int. J. Biochem. Cell Biol. 38 (2006) pp. 1092-1101.

[30] J.M. Patlolla, M.V. Swamy, J. Raju, C.V. Rao, Overexpression of caveolin-1 in experimental colon adenocarcinomas and human cancer cell lines, Oncol. Rep. 11 (2004) pp. 957-963.

[31] D. Merrick, L.K.J. Stadler, D. Larner, J. Smith, Muscular dystrophy begins early in embryonic development deriving from stem cells loss and disrupted muscle formation, Dis. Model. Mech. 2 (2009) pp. 374-388.

[32] F. Galbiati, D. Volonté, J.B. Chu, M. Li, S.W. Fine, M. Fu, J. Bermudez, M. Pedemonte, K.M. Weidenheim, R.G. Pestell, C. Minetti, M.P. Lisanti, Transgenic overexpression of caveolin-3 in skeletal muscle fibers induces a Duchenne-like muscular dystrophy phenotype, Proc. Natl. Acad. Sci. USA 97 (2000) pp. 9689-9694.

[33] K.H. Fischbeck, E. Bonilla, D.L. Schotland, Freeze-fracture analysis of plasma membrane cholesterol in Duchenne muscle, Ann. Neurol. 13 (1983) pp. 532-535.

[34] A. Pol, S. Martin, M.A. Fernández, M. Ingelmo-Torres, C. Ferguson, C. Enrich, R.G. Parton, Cholesterol and fatty acids regulate dynamic caveolin trafficking through the Golgi complex and between the cell surface and lipid bodies, Mol. Biol. Cell 16 (2005) pp. 2091-2105.

[35] A. Draeger, K. Monastyrskaya, F.C. Burkhard, A.M. Wobus, S.E. Moss, E.B. Babiychuk, Membrane segregation and downregulation of raft markers during sarcolemmal differentiation in skeletal muscle cells, Dev. Biol. 262 (2003) pp. 324-334.

[36] A. Draeger, K. Monastyrskaya, M. Mohaupt, H. Hoppeler, H. Savolainen, C. Allemann, E.B. Babiychuk, Statin therapy induces ultrastructural changes in skeletal muscle in patients without myalgia, J. Pathol. 210 (2006) pp. 94-102.

[37] K. Oexle and A. Kohlschütter, Cause of progression in Duchenne muscular dystrophy: impaired differentiation more probable than replicative aging, Neuropediatrics 32 (2001) pp. 123-129.

[38] N.P. Whitehead, E.W. Yeung, D.G. Allen, Muscle damage in *mdx* (dystrophic) mice: role of calcium and reactive oxygen species, Clin. Exp. Pharmacol. Physiol. 33 (2006) pp. 657-662.

[39] S. Fawzi-Grancher, R.J. Sun, M. Traore, J.F. Stoltz, S. Muller, Role of Ca^{2+} in the effects of shear stress and TNF-α on caveolin-1 expression, Clin. Hemorheol. Microcirc. 33 (2005) pp. 253-261.

[40] J. Liu, P. Oh, T. Horner, R.A. Rogers, J.E. Schnitzer, Organized endothelial cell surface signal transduction in caveolae distinct from glycosylphosphatidylinositol-anchored protein microdomains, J. Biol. Chem. 272 (1997) pp. 7211-7222.

[41] S. Ginés, F. Ciruela, J. Burgueño, V. Casadó, E.I. Canela, J. Mallol, C. Lluís, R. Franco, Involvement of caveolin in ligand-induced recruitment and internalization of A1 adenosine receptor and adenosine deaminase in an epithelial cell line, Mol. Pharmacol. 59 (2001) pp. 1314-1323.

[42] H.Q. Xie, R.C. Choi, K.W. Leung, N.L. Siow, L.W. Kong, F.T. Lau, H.B. Peng, K.W. Tsim, Regulation of a transcript encoding the proline-rich membrane anchor of globular muscle acetylcholinesterase. The suppressive roles of myogenesis and innervating nerves, J. Biol. Chem. 282 (2007) pp. 11765-11775.

[43] C. Legay, M. Huchet, J. Massoulié, J.P. Changeux, Developmental regulation of acetylcholinesterase transcripts in the mouse diaphragm: alternative splicing and focalization, Eur. J. Neurosci. 7 (1995) pp. 1803-1809.

[44] U. Salzer and R. Prohaska, Stomatin, flotillin-1, and flotillin-2 are major integral proteins of erythrocyte lipid rafts, Blood 97 (2001) pp. 1141-1143.

[45] E. Meshorer, D. Toiber, D. Zurel, I. Sahly, A. Dori, E. Cagnano, L. Schreiber, D. Grisaru, F. Tronche, H. Soreq, Combinatorial complexity of 5' alternative acetylcholinesterase transcripts and protein products, J. Biol. Chem. 279 (2004) pp. 29740-29751.

[46] D. Toiber, A. Berson, D. Greenberg, N. Melamed-Book, S. Diamant, H. Soreq, N-Acetylcholinesterase-induced apoptosis in Alzheimer's disease, PLoS ONE, Www. Plosone. Org 3 (2008) pp. 1-12.

[47] B. Li, J.A. Stribley, A. Ticu, W. Xie, L.M. Schopfer, P. Hammond, S. Brimijoin, S.H. Hinrichs, O. Lockridge, Abundant tissue butyrylcholinesterase and its possible function in the acetylcholinesterase knockout mouse, J. Neurochem. 75 (2000) pp. 1320-1331.

[48] V. Gisiger and H.R. Stephens, Localization of the pool of G_4 acetylcholinesterase characterizing fast muscles and its alteration in murine muscular dystrophy, J. Neurosci. Res. 19 (1988) pp. 62-78.

[49] F. Bacou, P. Vigneron, J. Massoulié, Acetylcholinesterase forms in fast and slow rabbit muscle, Nature 296 (1982) pp. 661-664.

[50] Z. Yablonka-Reuveni and J.E. Anderson, Satellite cells from dystrophic (mdx) mice display accelerated differentiation in primary cultures and isolated myofibers, Dev. Dynam. 235 (2006) pp. 203-212.

[51] H.Q. Xie, R.C.Y. Choi, K.W. Leung, V.P. Chen, G.K.Y. Chu, K.W.K. Tsim, Transcriptional regulation of proline-rich membrane anchor (PRiMA) of globular form acetylcholinesterase in neuron: an inductive effect of neuron differentiation, Brain Res. 1265 (2009) pp. 13-23.

[52] F. Stetzkowski-Marden, C. Gaus, M. Recouvreur, A. Cartaud, J. Cartaud, Agrin elicits membrane lipid condensation at sites of acetylcholine receptor clusters in C2C12 myotubes, J. Lipid Res. 47 (2006) pp. 2121-2133.

[53] I. Furlan and R. Oliveira-Godinho, Developing skeletal muscle cells express functional muscarinic acetylcholine receptors coupled to different intracellular signaling system, Br. J. Pharmacol. 146 (2005) pp. 389-396.

[54] J.A. Allen, R.A. Halverson-Tamboli, M.M. Rasenick, Lipid rafts microdomains and neurotransmitter signalling, Nat. Rev. Neurosci. 8 (2007) pp. 128-140.

[55] G. Johnson, C. Swart, S.W. Moore, Interaction of acetylcholinesterase with the G4 domain of the laminin alpha1-chain, Biochem. J. 411 (2008) pp. 507-514.

A)

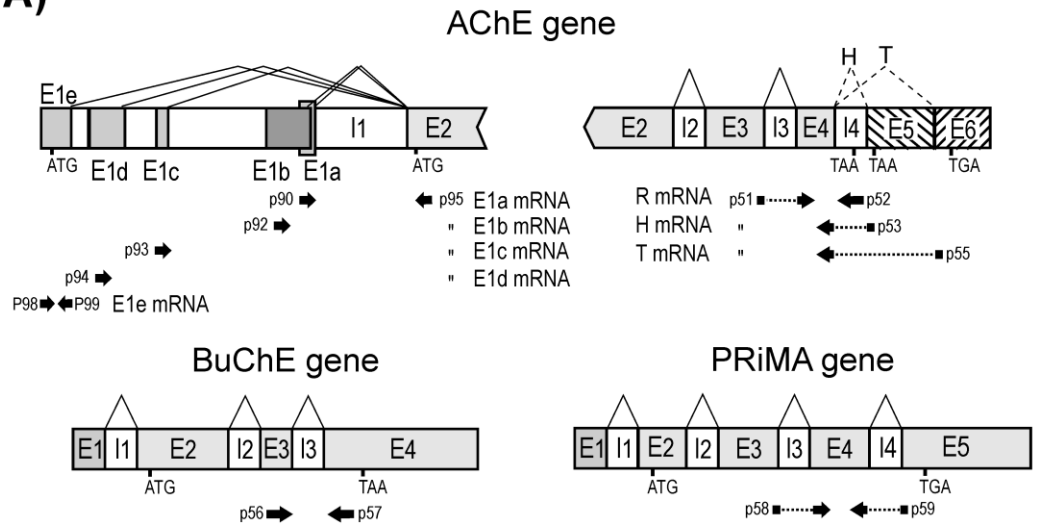

B)

	Forward Primers			Reverse Primers		
mRNA	**N°**	**Position**	**Sequence**	**N°**	**Position**	**Sequence**
AChE						
R	51	E3/E4	ATTT TGCC CGCA CAGG GGAC	52	I4	CCCC ACTC CATG CGCC TAC
H				53	E4/E5	AAGG AGCC TCCG TGGC GGT
T				55	E4/E6	CGCC TCGT CCAG AGTA TCGG T
E1a	90	E1a	AGCG GAGG GCAT TGCA ATA	95	E2	CCAG CAGC TGCG GGTC TTCC
E1b	92	E1b	TTTG ATCT CTTG GCTG GAGA CG			
E1c	93	E1c	GGAA CATT GGCC GCCT CCAG C			
E1d	94	E1d	CAGG CTGC GGTC CGTC TGTC A			
E1e	98	E1e	AAAG CTTG GCCC GGTG ATGT	99	E1e	AGCT CTGG AAAC TTCC GGA
Other mRNAs						
BuChE	56	E3	TAGC ACAA TGTG GCCT GTCT	57	E4	ATTG CTCC AGCG ATGA AATC
PRiMA	58	E3/E4	TACT CTCC GCCC CAGC TC	59	E4/E5	AGTG GTTT CCTC TTTA TGGC TTT
β-actin	34		AGAA AATC TGGC ACCA CACC	35		GGGG TGTT GAAG GTCT CAAA